NUMERICAL SIMULATION OF THE FLOWFIELD
OVER ICE ACCRETION SHAPES

IN-16766

SEMIANNUAL PROGRESS REPORT

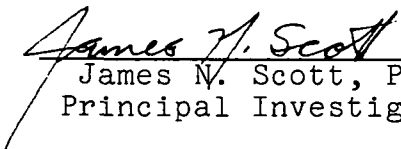### 30 October 1985 - 30 April 1986

c/s DE 333 333

Prepared For:

NASA Lewis Research Center
21000 Brookpark Road
Cleveland, Ohio 44135

Project Monitor: Dr. Robert J. Shaw

NASA Grant No. NAG 3-665

Submitted By:

James N. Scott, Ph.D.
Principal Investigator

University of Dayton
Research Institute
300 College Park
Dayton, Ohio 45469

NUMERICAL SIMULATION OF THE FLOWFIELD
OVER ICE ACCRETION SHAPES

1. INTRODUCTION

This is the first Semi-Annual Status Report submitted on Grant NAG 3-665. It includes the progress made during the period of October 1985 to April 1986. The NASA Technical Officer for this grant is Dr. Robert J. Shaw, NASA Lewis Research Center, Cleveland, Ohio.

2. R&D STATUS REPORT

The grant program schedule consists of five components, i.e., computer code revision, grid generation, computations, extraction of data, and report preparation. During this reporting period the first two components were accomplished and progress made on the computations. In addition, an abstract was prepared and submitted to the AIAA for potential presentation of these results at the Aerospace Sciences Meeting, January 12-15, 1987. Details of the program status follow in the next sections.

2.1 Technical Effort

In this section the progress of the technical effort will be discussed. The primary goals of this program are directed toward the development of a numerical method for computing flow about ice accretion shapes and determining the influence of these shapes on flow degradation. In pursuing these goals, it is expedient to investigate various aspects of icing independently in order to assess their contribution to the overall icing phenomena.

The specific aspects to be examined include the water droplet trajectories with collection efficiencies and phase change on the surface, the flowfield about specified shapes including lift, drag, and heat transfer distribution, and surface roughness effects. In treating these issues it must be kept in mind that they will ultimately be coupled together in a fashion which will permit accurate prediction of the complete icing process as well as

the influence on the surrounding flowfield. The following paragraphs describe the progress in examining these issues.

The first issue to address is the unsteady nature of the phenomenon.[1] Although the ice shape configuration changes with time, the rate of growth is slow (10^{-4} ft/sec) compared to the flight speed (200 ft/sec), therefore, a quasi-steady analysis is appropriate. This approach involves computation of Navier-Stokes solutions for a sequence of shapes starting from the original configuration, computing the growth rate, advancing the configuration over a fixed time interval (e.g., 50 sec), recomputing a new growth rate, etc., until the final period is attained.

A primary key to this approach is the accurate computation of the heat transfer over a roughened surface of unusual geometry. Although the Navier-Stokes equations conceptually possess the ability to simulate this process,[2] numerical confirmation has not yet been achieved. Fortunately, a series of experimental heat transfer tests have been accomplished[3,4,5,6] which assist in the validation of the computational fluid dynamic (CFD) methods. The purpose of this phase of the investigation is the computation of a series of these test cases to validate the numerical simulation.

The configurations computed were models of ice accretion shapes formed on a circular cylinder in the NASA Lewis Icing Research Tunnel (IRT). These shapes were 2-, 5-, and 15-minute models of glaze ice and a 15-minute accumulation of rime ice. An existing Navier-Stokes program was modified to compute the flowfield over these four shapes.

2.1.1 Governing equations

The governing equations are obtained by adding body forces to the Navier-Stokes equations to account for the drag of the droplet particles and surface roughness. In addition, a continuity and momentum equation are required to develop the trajectory equations for the droplets.

2

Air Equations

$$\frac{\partial \rho}{\partial t} + \nabla \cdot \rho \underline{V} = 0$$

$$\rho \frac{D\underline{V}}{Dt} = \nabla \cdot \underline{\underline{\tau}} \, \rho_p \underline{f}$$

$$\rho \frac{De}{Dt} = \nabla \cdot (\underline{\underline{\tau}} \cdot \underline{V} + \dot{\underline{q}}) \rho_p \underline{f} \cdot \underline{V}$$

Water Droplet Equations

$$\frac{\partial \rho_p}{\partial t} + \nabla \cdot \rho_p \underline{V}_p = 0$$

$$\frac{\partial \underline{V}_p}{\partial t} + \underline{V}_p \cdot \nabla \underline{V}_p = \underline{g} + \underline{f}$$

where

$$\underline{f} = \frac{C_D \rho S}{2m} |\underline{V} - \underline{V}_p|(\underline{V} - \underline{V}_p) = \text{droplet drag/unit mass}$$

The water droplets are assumed to be uniform spheres of diameter, d. Cloud physics experiments indicate d to vary between 5 and 50 microns depending upon the air temperature and liquid water content (see Aircraft Icing, NASA CP2086). Often an average value of 20 microns is used in ice accretion studies. Therefore,

$$\frac{\rho S}{2m} = \frac{\rho \pi d^2/4}{2\rho_w \pi d^3/6} = \frac{3\rho}{4\rho_w d}$$
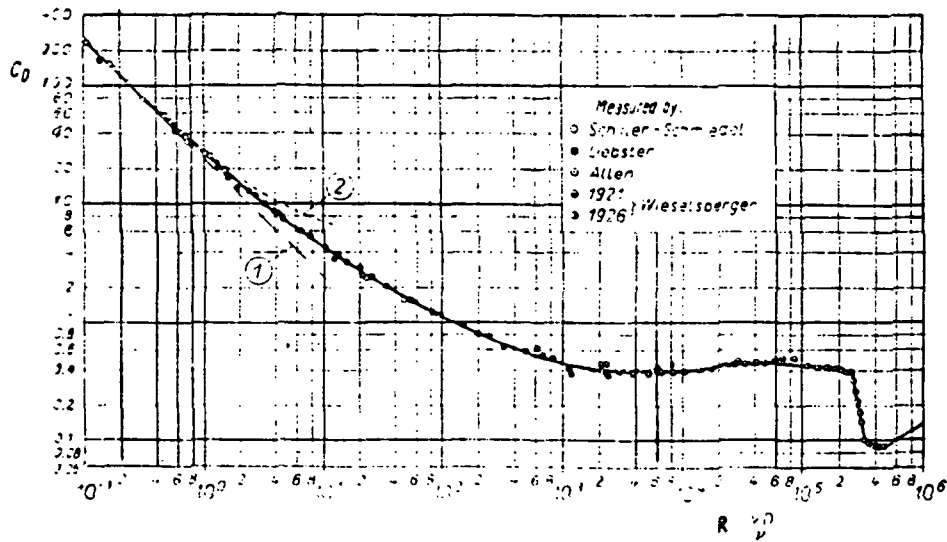
and

$$C_D = C_D(Re_d) \qquad \text{(see Figure 1)}$$

Figure 1. Drag Coefficient for Spheres as a Function of the Reynolds Number.

4

A curve fit of this classic plot produces the following:

$$Re_d < 1 \qquad\qquad C_D = \frac{24}{Re_d} \quad \text{(Stokes flow)}$$

$$1 < Re_d < 400 \qquad\qquad C_D = \frac{24}{(Re_d)^{0.646}}$$

$$400 < Re_d < 3 \times 10^5 \qquad C_D = 0.5$$

These values will be used in the computation of the water droplet trajectories.

2.1.2 Boundary conditions

Far field. At the far field boundary, the following conditions are prescribed:

$$\underline{V}_\infty, \quad T_\infty, \quad P_\infty$$

$$\rho_p = \text{LWC} = \text{liquid water content of cloud}$$

$$\underline{V}_p = \underline{V}_\infty$$

Surface. At the surface, the following conditions prevail:

$$\underline{V} = 0, \quad T_w \text{ specified} \qquad \frac{\partial p}{\partial n} = 0$$

2.1.3 Grid generation

The grid was developed using the hyperbolic grid generator of Steger and Barth. This technique appears ideally suited for computing grids for the irregular shapes of icing configurations. This method first requires a detailed description of the surface geometry. The program produces an orthogonal, body oriented grid (which is preferable in CFD computations) and clusters the grid points near the surface. The hyperbolic method

5

has little control over the final exterior grid shape, which is perfectly acceptable for external flow problems (but unacceptable for internal flows). An example grid is shown in Figure 2.

2.1.3.1 Solution of the water droplet equations

An efficient means for solving the water droplet trajectory equations was developed during this reporting period. Droplet trajectory equations in the past have been solved using the Lagrangian method. In this investigation it was proposed to use the Eulerian method for two reasons. First to make the droplet system of equations compatible with the airflow equations, and secondly to include the variation of the liquid water content (ρ_p) throughout the flowfield. The Lagrangian method presumes the water content to be constant.

The droplet equations are similar in form to the airflow equations with the exception that the stress tensor is zero. This difference, however, changes the mathematical character of the partial differential equations from elliptic to hyperbolic as will be shown in the following paragraph. This observation means that the hyperbolic equations may be marched in space using a Parabolized Navier-Stokes code (PNS). An advantage results in that the droplet equations may be solved in only a few seconds on a VAX computer.

2.1.3.2 Eigenvalue analysis of marching technique

The purpose of this section is to demonstrate the applicability of space-marching techniques to solve the governing fluid dynamic equations for water droplets motion. To correctly apply a space-marching technique the eigenvalues of the governing equations must be real (indicating the character of the equations is hyperbolic).

The governing equations in divergence form are written as:
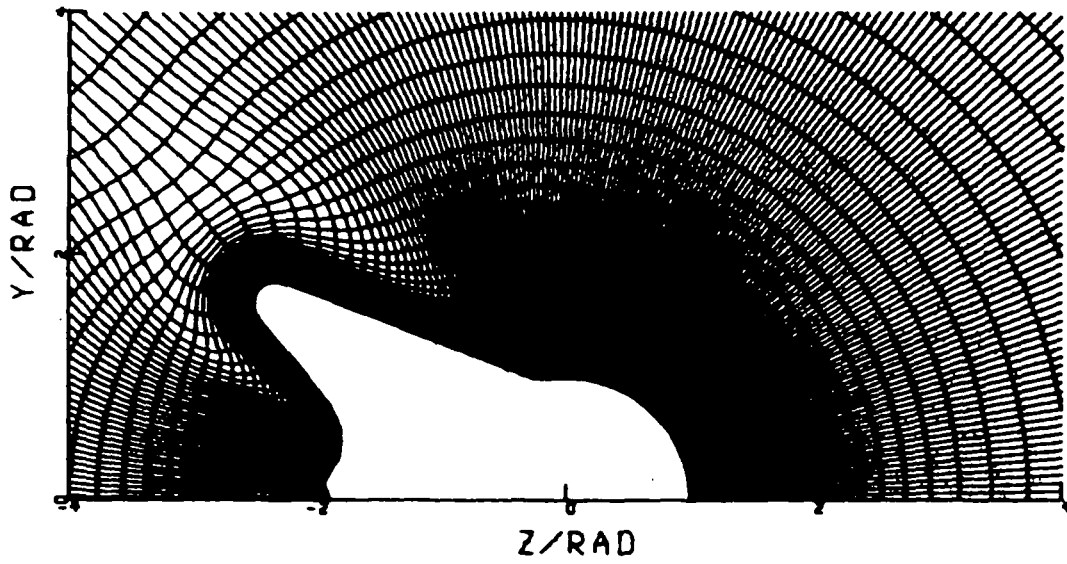
$$E_x + F_y = H$$

ICE GRID

Figure 2. Grid for 15-Minute Glaze Case.

where E, F, and H are defined by

$$E = \begin{bmatrix} \rho u \\ \rho u^2 \\ \rho uv \end{bmatrix} \qquad F = \begin{bmatrix} \rho v \\ \rho uv \\ \rho v^2 \end{bmatrix} \qquad H = \begin{bmatrix} 0 \\ -fx \\ -fy \end{bmatrix}$$

In order to perform the eigenvalue analysis the E and F vector are factored such that

$$E_x = \frac{\partial E}{\partial U} U_x = A U_x$$

$$F_y = \frac{\partial F}{\partial U} U_y = B U_y$$

where

$$U = \begin{vmatrix} \rho \\ u \\ v \end{vmatrix}$$

The A and B matrices are found to be

$$A = \begin{vmatrix} u & \rho & 0 \\ 0 & \rho u & 0 \\ 0 & 0 & \rho u \end{vmatrix}$$

$$B = \begin{vmatrix} v & 0 & \rho \\ 0 & \rho v & 0 \\ 0 & 0 & \rho v \end{vmatrix}$$

Applying the above factorization can be rewritten as

$$U_x + A^{-1} B U_y = A^{-1} H$$

To determine the character of this equation set it is necessary to find the eigenvalues of the matrix $\underline{A}^{-1}\underline{B}$. $\underline{A}^{-1}\underline{B}$ was found to be

$$\underline{A}^{-1}\underline{B} = \begin{vmatrix} \dfrac{v}{u} & \dfrac{-\rho v}{u^2} & \dfrac{\rho}{u} \\ 0 & \dfrac{v}{u} & 0 \\ 0 & 0 & \dfrac{v}{u} \end{vmatrix}$$

The characteristic equation of the matrix $\underline{A}^{-1}\underline{B}$ is determined from

$$\det[\underline{A}^{-1}\underline{B} - \lambda I] = 0$$

or in simplified form

$$\left(\frac{v}{u} - \lambda\right)^3 = 0$$

The eigenvalues of the matrix $\underline{A}^{-1}\underline{B}$ are defined as the roots of the characteristic equation. Therefore, the eigenvalues of $\underline{A}^{-1}\underline{B}$ are

$$\lambda = \frac{v}{u}$$

Since the eigenvalues are real, the character of the governing fluid dynamic equations is hyperbolic. Therefore, the governing equations can be solved with a hyperbolic space-marching scheme.

2.1.4 Solution procedure

The airflow was computed using a well documented Navier-Stokes code[14] adapted from the original program developed by Shang. The MacCormack algorithm is utilized and the program is vectorized for the CRAY computer. Also, the hyperbolic grid generator of Steger and Barth was used as discussed in the previous section. Since this portion of the project is current state of the art in CFD, little difficulty was encountered.

The computation of the droplet trajectories is computed using technology developed for the PNS solving schemes.

The droplet equations are hyperbolic since the stress-tensor vanishes for this model. (No collisions between droplets are considered in the formulation and hence no pressure or shear terms are present.) The governing equations are transformed into a ξ-η computational domain and take on the following form:

$$\begin{vmatrix} \rho_p V \\ \rho_p u_p V \\ \rho_p v_p V \end{vmatrix}_\eta = \begin{vmatrix} 0 \\ \dfrac{\rho_p(u_p - u)}{\tau J} \\ \dfrac{\rho_p(v_p - v)}{\tau J} \end{vmatrix} - \begin{vmatrix} \rho_p U \\ \rho_p u_p U \\ \rho_p v_p U \end{vmatrix}_\xi$$

where the contravariant velocity components are represented as

$$U = y_\eta u_p - x_\eta v_p$$

$$V = x_\xi v_p - y_\xi u_p$$

and

$$J^{-1} = \begin{vmatrix} x_\xi & x_\eta \\ y_\xi & y_\eta \end{vmatrix} \quad ; \quad \frac{4\rho_w d^2}{3 C_D Re_d \mu}$$

The upstream boundary conditions are

$$\rho_p(\infty) = LWC$$
$$u_p(\infty) = V_\infty$$
$$v_p(\infty) = 0$$

Given the air velocity components (u,v) from the solution of the airflow equations, the droplet equations are marched in the η-direction inward towards the body. After attaining the body surface the values of u_p, v_p, and ρ_p are recorded from which the local collection efficiency ($\bar{\beta}$) may be determined.

$$\bar{\beta} = \left(\frac{\rho_p}{LWC}\right)_w \left[\frac{u_p - v_p \cot\theta}{V_\infty}\right]_w$$

10

where tan $\theta = \left(\dfrac{dy}{dx}\right)_w$ = slope of the wall.

A dimensional analysis of the water droplet equations indicates that the collection efficiency is a function of the geometry and only one flow parameter, τ'; where

$$\tau' = \frac{V_\infty \tau}{R}$$

This single parameter is a type of Reynolds number, taking into account all flow variables of the problem, and is very useful for evaluating collection efficiencies. Figure 3 shows the sensitivity of $\bar{\beta}$ to τ' for various flows over circular cylinder.

2.2 Results

To calibrate the numerical procedure the heat transfer distribution over a smooth circular cylinder under laminar conditions was computed for which there exists an exact solution (Frössling[15]). Figure 4 shows a comparison of Nusselt number over a cylinder for the Navier-Stokes solution with the Frössling solution. Conditions for this case are $Re_d = 138,000$ and a diameter of 2 inches. Excellent agreement may be observed, proving the validity of the numerics.

Figure 5 shows the computed droplet velocity vector field around a 2-inch diameter cylinder in potential flow with a free stream velocity of 130 fps.

Preliminary computations of the flowfield about each of the ice shapes have been performed. Refinement of these computations are currently being examined in order to achieve the required accuracy.
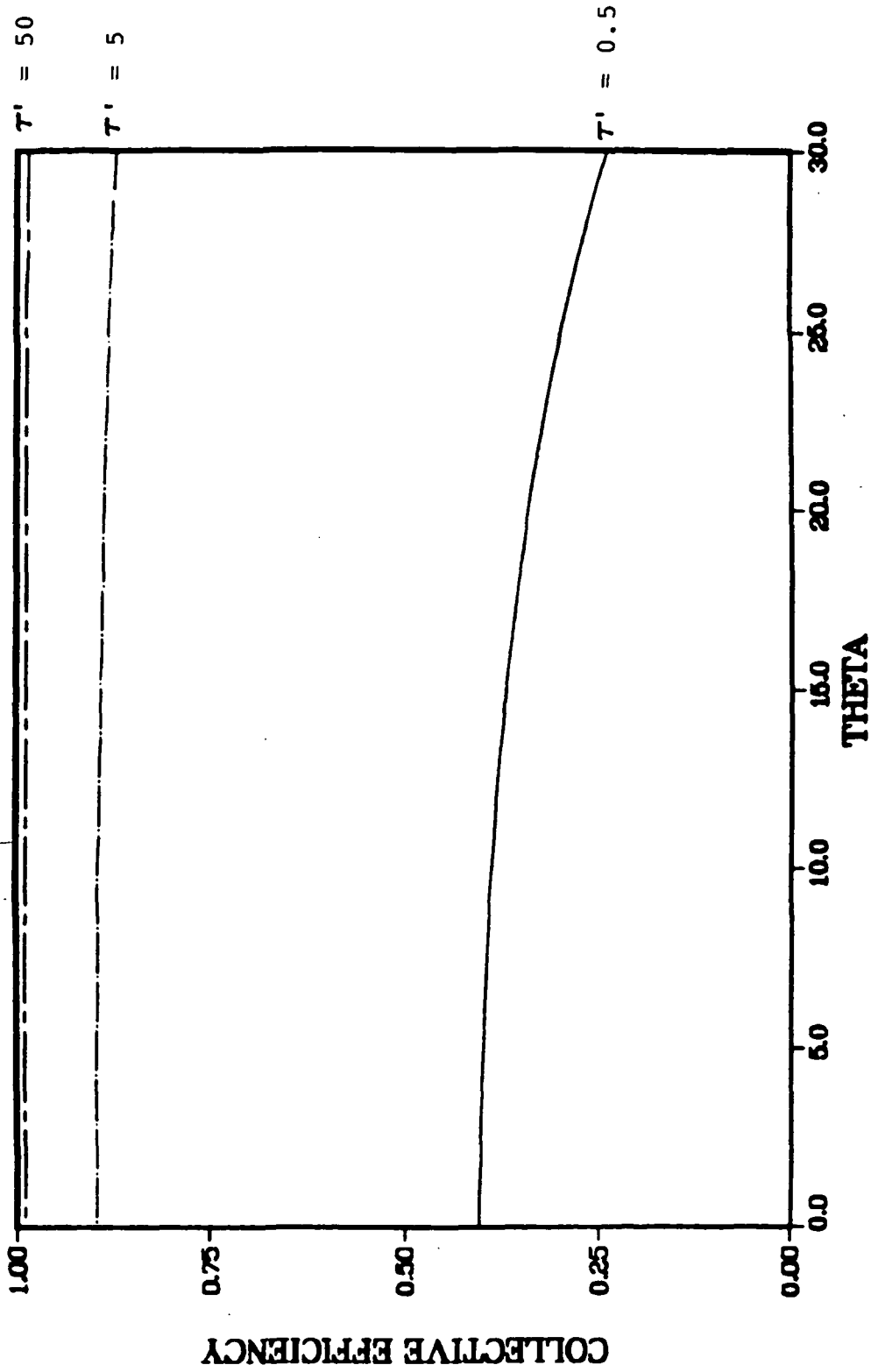
Figure 3. Computed Collection Efficiences for Various τ' Values for Cylinder.
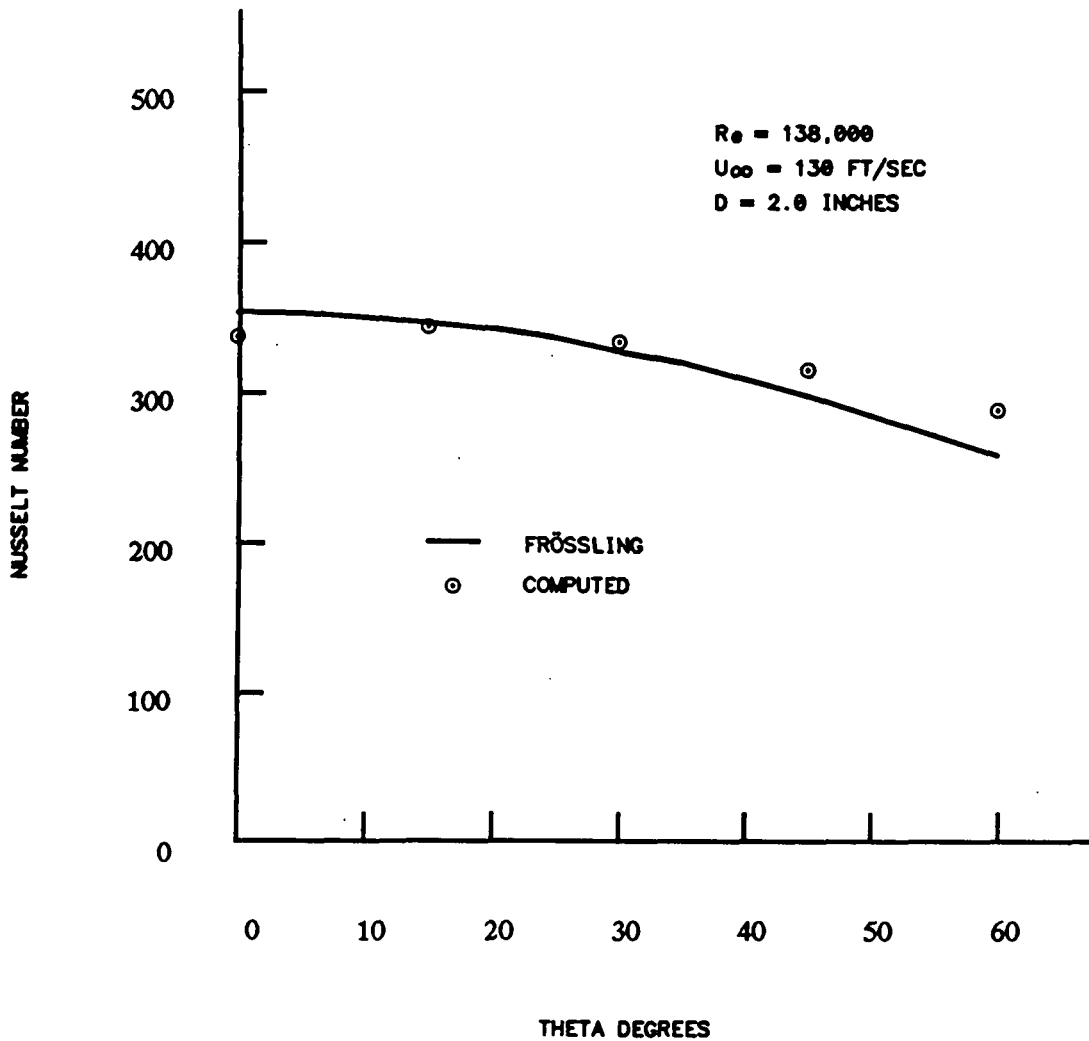
Figure 4. Comparison of Computed Nusselt Number
          Distribution with Frössling Solution.

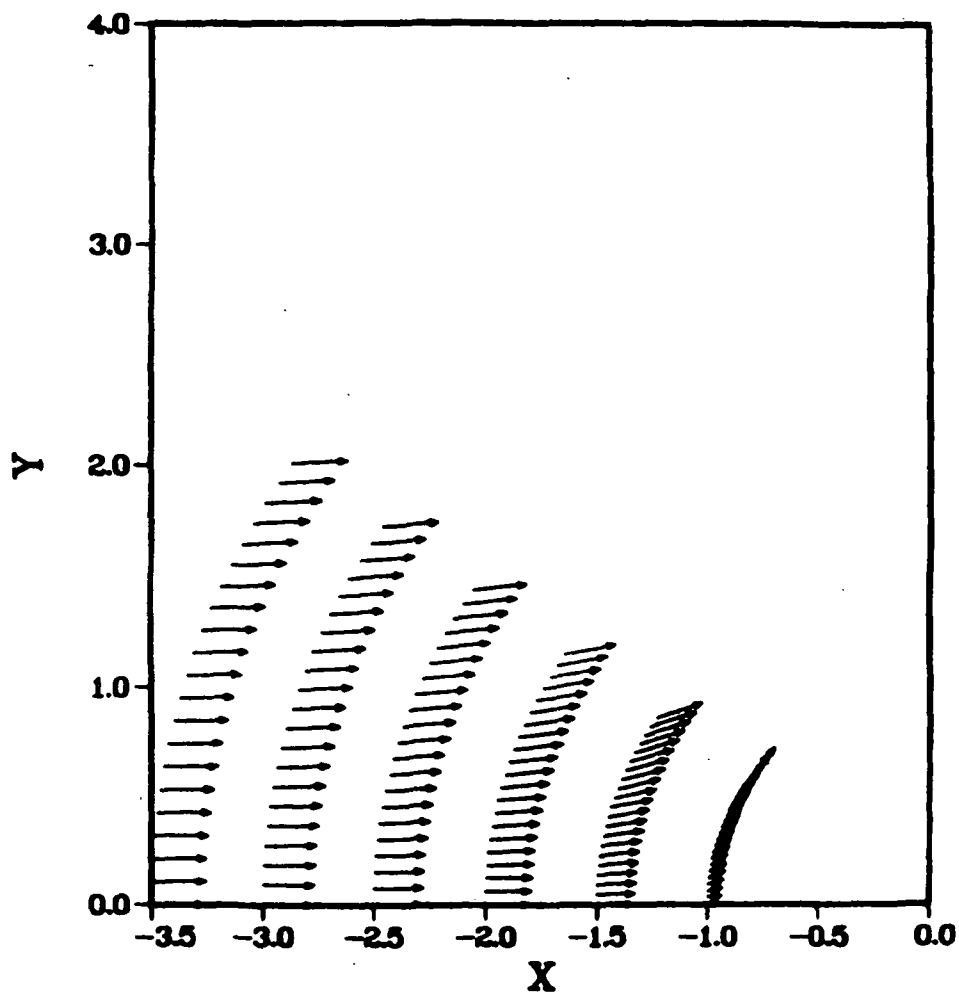# COMPUTED DROPLET VELOCITY VECTORS

Figure 5.   Computed Droplet Velocity Vectors
            Over a Cylinder $\tau' = 0.476$.

References

1. Shaw, R. J., "Progress Toward the Development of an Aircraft Icing Analysis Capability," NASA TM 83562, Jan. 1984.

2. Potapczuk, M. G. and Gerhart, P. M., "Progress in development of a Navier-Stokes Solver for Evaluation of Iced Airfoil Performance, AIAA Paper 85-0410, Jan. 1985.

3. Van Fossen, G. J. Simoneau, R. J., Olsen, W. A., and Shaw, R. J., "Heat Transfer Distributions Around Nominal Ice Accretion Shapes Formed on a Cylinder n the NASA Lewis Icing Research Tunnel, AIAA paper 84-0017, Reno, Nevada, Jan. 1984.

4. Pais, M. and Singh, S. N., "Determination of the Local Heat Transfer Coefficients of Three Simulated Smooth Ice Formation Characteristics on a Cylinder," AIAA Paper, Snowmass, Colorado, Aug. 1985.

5. Smith, M. E., Arimilli, R. V., and Keshock, E. G., "Measurement of Local Convective Heat Transfer Coefficients of Four Ice Accretion Shapes," NASA Contract Report 174680, May 1984.

6. Bragg, M. B. and Coirier, W. J., "Detailed Measurements of the Flow Field in the Vicinity of an Airfoil with Glaze Ice," AIAA Paper 85-0409, Jan. 1985.

7. Langmuir, I. and Blodgett, K. B., "A Mathematical Investigation of Water Droplet Trajectories," AAF-ATSC Tech. Report 5418, Feb. 1946.

8. Bragg, M. B., "Rime Ice Accretion and Its Effect on Airfoil Performance," NASA Contractor Report 165599, March 1982.

9. Bragg, M. B., Zaguli, R. J., and Gregorek, G. M., "Wind Tunnel Evaluation of Airfoil Performance Using Simulated Ice Shapes," NASA Contractor Report 167960, Nov. 1982.

10. Zaguli, R. G., Bragg, M. B., and Gregorek, G. M., "Results of an Experimental Program Investigating the Effects of Simulated Ice on the Performance of the NACA 63A415 Airfoil with Flap," NASA Contractor Report 168188, Jan. 1984.

11. Messinger, B. L., "Equilibrium Temperature of an Unheated Icing Surface as a Function of Airspeed," Journal of Aeronautical Sciences, Vol. 20, Jan. 1953.

12. Hankey, W. L. and Kirchner, R., "Ice Accretion of Wing Leading Edges," AFFDL TM-79-85-FXM, June 1979.

13. MacArthur, C. D., "Numerical Simulation of Airfoil Ice Accretion," AIAA Paper 83-0112, Jan. 1983.

14. Scott, J. N. and Hankey, W. L., "Numerical Simulation of Cold Flow in an Axisymmeric Centerbody Combustor," _AIAA Journal_, Vol. 23. No. 5, May 1985.

15. Frössling, N.; NACA Tech Memo 1432.

APPENDIX

Description and Use of HGRID

Hyperbolic Grid Generator

HGRID has a nicely structured modular form. Though it is not completely clear to the uninformed observer just what each subroutine does, the important routines are easily identifiable. Much of the code should be considered a "black box". The routines which you will most likely want to change are the main program, BODIS, and INITIA. These sections of the program involve setting up the body, defining important parameters such as loop sizes and output of the grid. A list of the primary subroutines and their purpose is shown below in order of appearance in the code.

MAIN   — Output of the completed grid.

SARC   — Called at each arc by STEP, sets up integration parameters based on input parameters and scaling factors.

BODIS   — Reads in or generates the body coordinates, called by INITIA.

INITIA — Reads in or assigns the smoothing and integration input parameters, sets up stretching and scaling factors based on the input parameters, called by MAIN.

METRIC — Generates the coordinate transformation metrics for the integration, called at each arc by STEP.

STEP   — Marches the grid generation out from the body. Calculates X, Y coordinates at next arc, called by MAIN.

VOLUME — Calculates the "volume" or area of each cell formed by the present arc and where the new arc should lie based on variable scaling factors. Called by STEP.

The basic procedure in the process of grid generation is as follows:

1) Body coordinates and input parameters are read, and the body coordinates are written to the output file.

2) STEP is called and it calls routines to set up: integration parameters, cell areas and the right hand side of the PDE to be solved.

3) The PDE is solved by routines called by STEP, and within STEP the X, Y values for the next arc are calculated.

17

4) In MAIN, the X, Y values of the new arc are written to tape, and STEP is called again.

The sequence of calculating the next arc out from the body and then writing it to tape eliminates the need to store X and Y in two dimensional arrays. This cuts down on the memory required by HGRID.

Changes to HGRID will most likely be changes in the body coordinates, loop sizes and final grid form. These changes will all take place in MAIN, BODIS and INITIA. The other input parameters defined in INITIA should be considered constants that need not be changed. They have been found to work well for many grid generation cases. Two factors, however, that you may wish to control are DSETA and ESCAL. DSETA is the initial step size out from the body in eta, the transformed coordinate normal to the body. ESCAL controls the scale factor that is used to calculate the cell areas or volumes.

Hint: In the event that only the upper or lower half of a grid is needed due to symmetry conditions, you must supply HGRID with the whole set of body coordinates anyway. For HGRID to function, it needs to be given a complete, closed body. You can cut the mesh in half after the complete grid has been generated.